Biomedicine & Pharmacotherapy 193 (2025) 118750

Contents lists available at ScienceDirect

Biomedicine & Pharmacotherapy

journal homepage: www.elsevier.com/locate/biopha

Endogenous gut microbiome and implanted intranasal *E. coli-Nissle* modulate cancer tissues metabolism in 4T1 syngeneic tumor bearing mice

Alexander Cecil [a,*,1], Ivaylo Gentschev [b,1], Cornelia Prehn [a], Stefanie Hauck [a], Michael Witting [a], Ivan Petrov [b], Mingyu Ye [b], Eman M. Othman [b,**], Aladar A. Szalay [b,c,d,**]

[a] Helmholtz Zentrum München, German Research Center for Environmental Health (GmbH), Metabolomics & Proteomics Core, Neuherberg 85764, Germany
[b] Department of Biochemistry/Cancer Therapy Research Center (CTRC), Theodor-Boveri-Institute, University of Wuerzburg, Wuerzburg 97074, Germany
[c] Department of Radiation Oncology, Rebecca & John Moores Comprehensive Cancer Center, University of California, San Diego, CA 92093, USA
[d] Department of Pathology, Center of Immune Technologies, Stanford University School of Medicine, Stanford, CA 94305, USA

ARTICLE INFO

Keywords:
Anticancer
Gut microbiome
E. coli Nissle
4T1 syngeneic tumor

ABSTRACT

Despite recent progress in the diagnosis and treatment of advanced cancers, the overall patient treatment outcome did not substantially improve over the last years. Therefore, developing novel therapies, which may also work synergistically in combination with the conventional therapies is crucial. One promising new therapeutic approach is bacterium-mediated cancer therapy. In the current work, we describe the influence of the gut microbiome and intranasal E. coli Nissle applications on the metabolism in cancer tissues of 4T1 syngeneic tumor bearing mice. Here we found that after gut microbiome depletion and/or E. coli Nissle treatment the ratios of ADMA/Arginine, Putrescine/Ornithine and Kynurenine/Tryptophan as well as the total concentration of Carnosine, Kynurenine and H1 (synonymus for all sugars detectable) are significantly altered in tumor tissues of as the result of treatment. In conclusion, our current data show that E. coli Nissle bacteria facilitating metabolic modulation of tumors, a finding could be important for improved cancer therapy in patients.

1. Introduction

Cancer remains one of the leading causes of mortality worldwide [1], and despite advances in conventional treatments such as surgery, radiation, and chemotherapy, therapeutic options for patients with advanced-stage disease remain limited, often resulting in poor clinical outcomes. This underscores the urgent need for novel therapeutic strategies that can complement or enhance existing modalities. One promising therapeutic approach is bacterium-mediated cancer therapy [2,3]. The most important challenges for the successful clinical use of bacteria are ensuring their preferential tumor colonization and initiating functional tumor-specific immunity [4]. Several different bacteria, including *Salmonella* spp. [5], *Bifidobacterium longum* [6], *Eschericha coli* [7], *Listeria monocytogenes* [8] and *Clostridium spp.* [9,10] have been tested as anticancer agents in preclinical studies [11–13]. Unfortunately, only a limited number of bacterial strains have undergone successful testing in human clinical trials involving cancer patients. The Escherichia coli Nissle 1917 (EcN) strain, which has probiotic properties, is one of the new and promising candidates for bacterium-mediated cancer therapy [14]. This non-pathogenic EcN is the basis for an edible drug called "Mutaflor"® (Ardeypharm, Germany), which is utilized for the treatment and prevention of gastrointestinal disorders, including ulcerative colitis [15], chronic constipation [16], Crohn's disease [17] and irritable bowel syndrome [18]. Several engineered variants of EcN for treatment of metabolic disorders [19], infectious diseases [20] and cancers are currently in Phase I clinical trials. In addition, it was shown that the Nissle strain has immunomodulatory effects; for example, it suppresses immune-mediated damage and upregulates beneficial responses [21]. Furthermore, our group as well as others have previously demonstrated the ability of EcN to preferentially colonize tumor tissues [22–26]. Very recently, we analyzed the impact of the gut microbiome on the antitumor capacity of an EcN derivate strain (EcN/pMUT-gfp Knr) [27] in

* Corresponding author.
** Corresponding authors at: Department of Biochemistry/Cancer Therapy Research Center (CTRC), Theodor-Boveri-Institute, University of Wuerzburg, Wuerzburg 97074, Germany.
E-mail addresses: alexander.cecil@helmholtz-munich.de (A. Cecil), eman.sholkamy@uni-wuerzburg.de (E.M. Othman), a.szalay_ctrc@uni-wuerzburg.de (A.A. Szalay).
[1] These authors contributed equally to this work

https://doi.org/10.1016/j.biopha.2025.118750
Received 11 September 2025; Received in revised form 31 October 2025; Accepted 7 November 2025
Available online 15 November 2025

4T1 mammary carcinoma-bearing BALB/c mice [28]. The gut microbiome is a collection of diverse microorganisms, such as bacteria, fungi, and archaea, which normally reside within the gastrointestinal tract [29–31]. Gut microbiota can have opposing functions from pro-tumorigenic to anti-tumorigenic effects [30–32]. As a result, the possible role of the gut microbiota in cancer treatment of different cancer types is currently under an intensive investigation.

This manuscript aims to conduct a preclinical translational investigation into the metabolic effects of the probiotic Escherichia coli Nissle (EcN) and microbiome depletion within a murine tumor model. The research employs comprehensive metabolomic profiling to characterize metabolic changes associated with tumors that result from microbiome modulation, using the 4T1 syngeneic breast cancer model. The study stresses the importance of recognizing broad metabolic changes that indicate how microbial interventions affect tumor metabolism, rather than outlining a particular molecular mechanism.

In this study we analysed metabolite profiles in cancer tissues of 4T1 syngeneic tumor bearing mice after temporal antibiotic-induced depletion of the gut microbiome and/or intranasal Escherichia coli Nissle 1917 (EcN) treatments. Our findings demonstrate that both antibiotic-induced, temporal depletion of the gut microbiome and intranasally applied bacterial treatment lead to statistically significant metabolite changes in the cancer tissues compared that of the control animals. These findings may be helpful for the design of new diagnosis and therapeutic approaches for cancer therapy with EcN and offer proof-of-concept evidence that supports the promise of microbiome-driven metabolic modulation as a basis for future translational cancer therapies.

2. Materials and methods

The bacterial strain EcN/pMUT-gfp Kn^r [26] is a derivate of *E. coli* Nissle 1917 (Ardeypharm GmbH, Herdecke, Germany) carrying a kanamycin (Kn)-resistance cassette as well as a green fluorescent protein (GFP) gene. Here, the strain EcN/pMUT-gfp Kn^r was grown in Luria Bertani (LB) Broth medium (Sigma-Aldrich-L3022, Schnelldorf, Germany) containing 30 μg/mL kanamycin (Sigma-Aldrich, Schnelldorf, Germany). Bacteria were harvested and washed with endotoxin-free, sterile phosphate-buffered saline (PBS) (Dulbecco, Sigma-Aldrich, Germany, cat. No.: TMS-012-A) prior to injection.

The 4T1 mammary cancer cells (ATCC: CRL-2539) were cultured in DMEM medium (Thermo Fisher Scientific, Schnelldorf, Germany, 11965092) supplemented with 10 % fetal bovine serum (FBS; Sigma-Aldrich, Schnelldorf, Germany, F4135) and 1 % penicillin-streptomycin antibiotic solution (Sigma-Aldrich, Schnelldorf, Germany, P4333) at 37 °C in a humidified incubator with 5 % CO_2.

2.1. Antibiotic-induced microbiome depletion in mice

For gut microbiome depletion, BALB/c mice (Charles River, Sulzfeld, Germany) received a cocktail of four antibiotics and one antimycotic [ampicillin 1 g/L (Sigma-Aldrich, Schnelldorf, Germany, A9518), vancomycin 0,35 g/L (Sigma-Aldrich, Schnelldorf, Germany, V2002), neomycin 1 g/L (Sigma-Aldrich, Germany, N1876), metronidazole 1 g/L (Sigma-Aldrich, Schnelldorf, Germany, M1547) and amphotericin B 0.1 g/L (Sigma-Aldrich, Schnelldorf, Germany, A2942)] in their drinking water, as described in previous reports [33,34]. The antibiotic cocktail was administered to mice for a period of 7 days and was replaced every other day. At days 4 and 7 after antibiotic treatment (ABT), faecal samples of antibiotic-treated mice were collected and analyzed as already described by Gentschev et al., 2022 [28].

- **Tumor treatment with the E. coli Nissle strain (EcN/pMUT-gfp Kn^r) in 4T1 tumor-bearing BALB/c mice**

Animal experiments were carried out in accordance with the protocol approved by the Government of Upper Franconia, Germany, according to the guidelines for the welfare and use of animals in cancer research (application No.: RUF-55.2.2.–2532–2–849).

The tumors were generated by implanting 1×10^5 mammary carcinoma 4T1 cells subcutaneously into the right dorsal flank regions of 5- to 6-week-old female BALB/c mice (Charles River, Sulzfeld, Germany). When tumors reached 100–250 mm^3, four groups of mice (n = 5), two antibiotic-treated (ABT) and two untreated, were injected intranasally (i.n.) twice either with EcN/pMUT-gfp Kn^r (1×10^7 bacteria/15 μL PBS/mouse) or with PBS only (15 μL PBS per mouse). During treatment, the tumor volume of each mouse was determined with a digital caliper at least two times per week and calculated by use of the modified ellipsoid formula [(length × width2)/2].

2.2. Analysis of bacterial colony forming units (CFU) in tumor samples

To determine bacterial load in tumor tissues, the EcN/pMUT-gfp Kn^r treated mice were euthanized and the tumors were excised, weighed and homogenized in sterile PBS. The homogenates were serially diluted and plated on LB agar plates containing 30 μg/mL kanamycin (Sigma-Aldrich, Schnelldorf, Germany, B5264). Resultant colonies were counted, and the bacterial numbers were calculated as CFU per 1 g tumor tissue.

2.3. Preparation of tumor samples for metabolomics

For metabolomics studies of different treated 4T1 tumor-bearing BALB/c mice, tumors were excised, snap-frozen in liquid nitrogen and then used for metabolomics analyses.

2.4. Metabolomics

Targeted metabolomics measurements were performed using liquid chromatography- and flow injection-electrospray ionization-tandem mass spectrometry (LC- and FIA-ESI-MS/MS) and the Absolute*IDQ*™ p180 Kit (BIOCRATES Life Sciences AG, Innsbruck, Austria). The assay allows simultaneous quantification of 188 metabolites out of plasma or tissue homogenate. The complete assay procedures as well as the tissue extraction in principle have been previously published [35]. For this type of murine tumor tissue samples, the tissue extraction method has been adapted specifically. In brief, tissue homogenates were always prepared freshly as follows:

Frozen murine tumor tissue samples were weighted into homogenization tubes with ceramic beads (1.4 mm). For metabolite extraction, to each 1 mg of frozen murine tumor tissue, 3 μL of a 4 °C cooled mixture of ethanol/phosphate buffer (85/15 v/v) were added. Tissue samples were homogenized using a Precellys24 homogenizer (PEQLAB Biotechnology GmbH, Germany), 3 x for 30 s at 5500 rpm and −4 °C, with 30 s pause intervals to ensure constant temperature, followed by centrifugation at 10,000 x g for 5 min. Subsequently, 5 μL of the supernatants were placed into the cavities of the 96-well filter plate of the p180 assay. Samples were dried in a nitrogen stream for 30 min. Amino acids and biogenic amines in the samples were derivatized with an excess of 5 % phenylisothiocyanate for 20 min and dried in a nitrogen stream. Samples were extracted for 30 min at RT with 300 μL methanol containing 5 mM ammonium acetate. The LC run was performed using an Agilent XDB-C18 column (3 ×100 mm, 3.5 μm). Sample handling was performed by a Hamilton Microlab STAR™ robot (Hamilton Bonaduz AG, Bonaduz, Switzerland) and a Ultravap nitrogen evaporator (Porvair Sciences, Leatherhead, U.K.), beside standard laboratory equipment. Mass spectrometric analyses were done on an API 4000 triple quadrupole system (SCIEX Deutschland GmbH, Darmstadt, Germany) equipped with a 1260 Series HPLC (Agilent Technologies Deutschland GmbH, Böblingen, Germany) and a HTC-xc PAL auto sampler (CTC Analytics, Zwingen, Switzerland) controlled by the software Analyst 1.6.2. For the LC-part, compounds were identified and quantified based on scheduled

multiple reaction monitoring measurements (sMRM), for the FIA-part on MRM. Data evaluation for quantification of metabolite concentrations and quality assessment were performed with the software MultiQuant 3.0.1 (SCIEX) and the Met*IDQ*™ software package, which is an integral part of the Absolute*IDQ*™ Kit. Metabolite concentrations were calculated using internal standards and reported either in pmol/mg for wet tissue or μmol/L (μM) for tissue homogenate.

2.5. Statistical analyses

Statistical analyses were prepared with R (vers. 4.2.1) and metaboanalyst (vers. 5.0 [35]). R scripts were used to detect missingness and for general quality control of the metabolites and samples. NA detection was performed and the metabolites c4(OH)Pro, DOPA, Dopamine, Nitro/Tyr, SDMA, PC ae C42:4, SM C20:2 and SM C22:3 had to be excluded as they had more than 40 % of NA over all samples and where thus deemed to unreliable. CV testing was also performed and C14:1-OH, C16:1-OH, C16:2, C16-OH, C3:1, C5:1-DC, C5-DC (C6-OH), C6:1, C7-DC, C9, Histamine, PC ae C30:1, Spermine, lysoPC a C26:0 and lysoPC a C26:1 were removed due to a coefficient of variation (CV) of more than 25 %. PLS-DAs were used to prepare a general overview of the data. Further detailed analyses were prepared as follows:

All remaining metabolites (after QC) from the Absolute*IDQ*™ p180 Kit, which have an inherent left shift of measured concentrations, were then transformed to normal data distribution by normalizing the samples by sum, log tranformation as well as pareto scaling of the measured values. ANOVA was applied to elucidate the significant changes over all the different groupings in the data and those which passed Fisher's posthoc were then used to prepare volcano plots and pathway analyses. The groupings of data are as follows: For gut microbiome depletion and E. coli Nissle (EcN/pMUT-gfp Kn^r) injections, 4T1 tumor-bearing BALB/c mice were treated with either an antibiotic cocktail (ABT), PBS, bacteria (EcN) or combinations thereof, as described in the Materials and Methods. During the treatment the tumor volume of each mouse was determined at least two times per week. Mice of all treated groups (PBS, ABT PBS, EcN, and ABT EcN) were euthanized before achievement of an excessive tumor burden (>1500 mm^3), as requested by the animal protocol. After that the tumors were excised and used for metabolomics analyses.

3. Results

PLS-DA of the homogenized tumor tissue samples revealed a clear metabolic separation between EcN-treated and PBS-treated groups, irrespective of antibiotic pre-treatment. The model showed strong performance with an R^2Y of 0.774, R^2X of 0.629, and a Q^2 of 0.505 (Fig. 1A). A parallel analysis of the directly measured, non-homogenized tissue samples yielded nearly identical results ($R^2Y = 0.775$, $R^2X = 0.631$, $Q^2 = 0.509$; Fig. 1B), using the same PLS-DA settings. Both models were validated using 10-fold cross-validation and 2000-fold permutation testing, with highly significant p-values ($p = 5 \times 10^{-4}$) for both permuted R^2 and Q^2 metrics. Together, these results confirm the robustness of the observed metabolic distinction induced by EcN treatment, regardless of sample preparation method.

(A) Partial Least Squares Discriminant Analysis (PLS-DA) of homogenized tumor tissue samples reveals clear metabolic separation between PBS-treated (purple and green) and E. coli Nissle (EcN)-treated (red and blue) groups, independent of antibiotic pre-treatment. The model demonstrates strong classification performance with $R^2Y = 0.774$, $R^2X = 0.629$, and $Q^2 = 0.505$.

(B) A comparable separation is observed in non-homogenized, directly measured tumor tissues, with nearly identical model statistics: $R^2Y = 0.775$, $R^2X = 0.631$, and $Q^2 = 0.509$.

Both models were rigorously validated using 10-fold cross-validation and 2000-fold permutation testing, yielding significant model robustness with p-values of 5×10^{-4} for permuted R^2 and Q^2 in both analyses. These results confirm that EcN treatment induces reproducible and distinct metabolic shifts in tumor tissues across both sample preparation methods.

As expected from the strong PLS-DA clustering, no major differences were observed between homogenized and non-homogenized tissue samples, regardless of antibiotic treatment. However, the metabolic differences between EcN-treated and non-EcN (PBS) groups were striking and consistent across both sample types. These patterns were further supported by statistical testing using ANOVA with false discovery rate (FDR) correction, which highlighted a distinct set of significantly altered metabolites in EcN-treated versus control groups, irrespective of tissue homogenization status (suppl. Table 1a, with its power calculation in suppl. Table 1b). These statistically relevant metabolites were

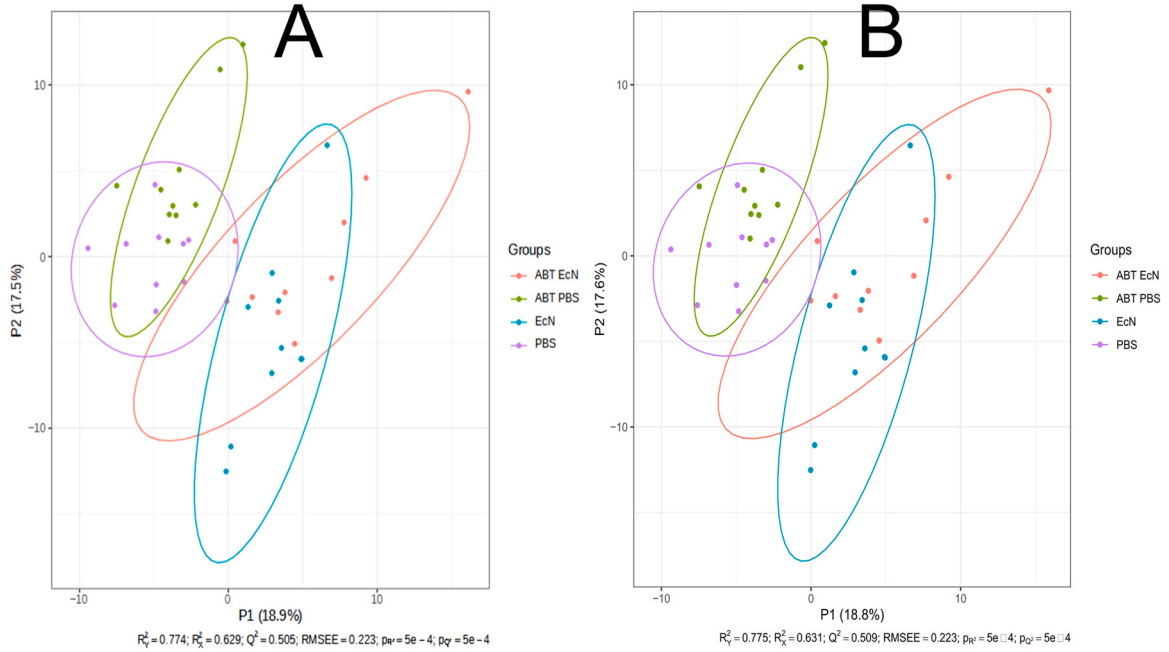

Fig. 1. PLS-DA of metabolomic profiles from homogenized and direct tumor tissue samples.

subsequently subjected to pathway enrichment analysis using MetaboAnalyst [35].

For the pathway analyses significantly affected metabolites from suppl. table 1a were chosen for pairings of ABT EcN vs ABT PBS and EcN vs PBS.

The resulting pathway analysis suggest that the statistically significant metabolite changes of the tissue samples are mainly located in the Oxidation of Branched Chain Fatty Acids, Urea Cycle, Beta Oxidation of Very Long Chain Fatty Acids, Arginine and Proline Metabolism. The Tryptophan Metabolism and the Beta-Alanine Metabolism show a raw p-value of < 0.05 in the tissue samples without antibioitcs only.

The homogenate samples show also a rather similar pattern, however there are some more differences between the pathway analyses of the antibiotic and non-antibiotic groups. The Spermidine and Spermine Biosynthesis, Methionine Metabolism, Glycine and Serine Metabolism, Arginine and Proline Metabolism, D-Arginine and D-Ornithine Metabolism, Tryptophan Metabolism, Betaine Metabolism, Oxidation of Branched Chain Fatty Acids and Urea Cycle are similarly found to be significantly affected in both groups by their raw p-value. However Alanine Metabolism, Glutathione Metabolism, Ammonia Recycling, Porphyrin Metabolism, Glutamate Metabolism, Carnitine Synthesis, Bile Acid Biosynthesis and Purine Metabolism are only found to be below 0.05 in the raw p-value in the homogenate samples without antibiotic, whereas Thyroid hormone synthesis, Catecholamine Biosynthesis, Tyrosine Metabolism, Valine, Leucine and Isoleucine Degradation, Phenylalanine and Tyrosine Metabolism and Propanoate Metabolism are exclusively below 0.05 (raw p-value) for the homogenate samples with antibiotics. (Figs. 2–5 and Spp.Tables 2–5).

This analysis identifies metabolic pathways significantly impacted by intranasal administration of E. coli Nissle (EcN) in homogenate samples without prior antibiotic treatment. Pathways showing significant enrichment (raw p-value < 0.05) include Spermidine and Spermine Biosynthesis, Methionine Metabolism, Glycine and Serine Metabolism,

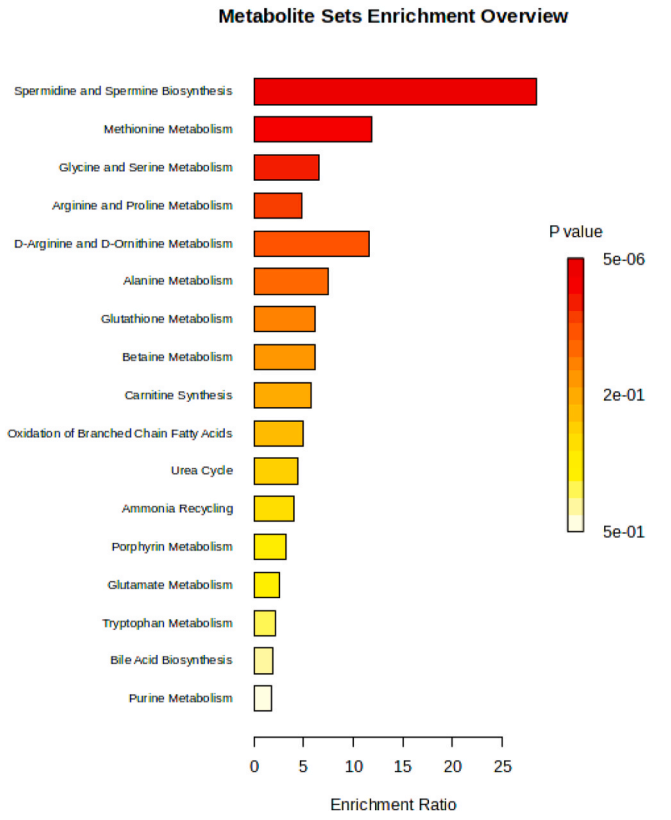

Fig. 2. Pathway enrichment analysis of homogenate samples comparing EcN vs PBS.

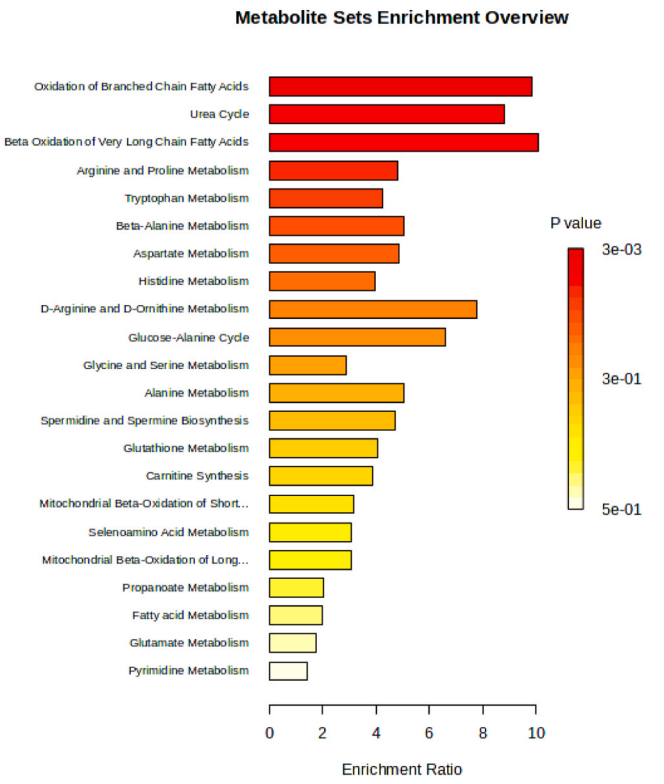

Fig. 3. Pathway enrichment analysis of tissue samples comparing EcN vs PBS.

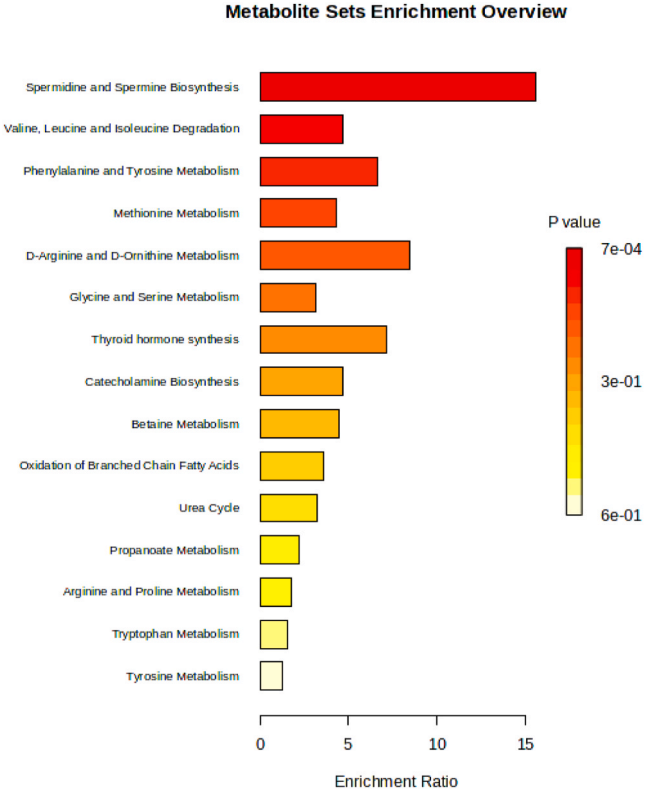

Fig. 4. Pathway enrichment analysis of homogenate samples comparing ABT EcN vs ABT PBS.

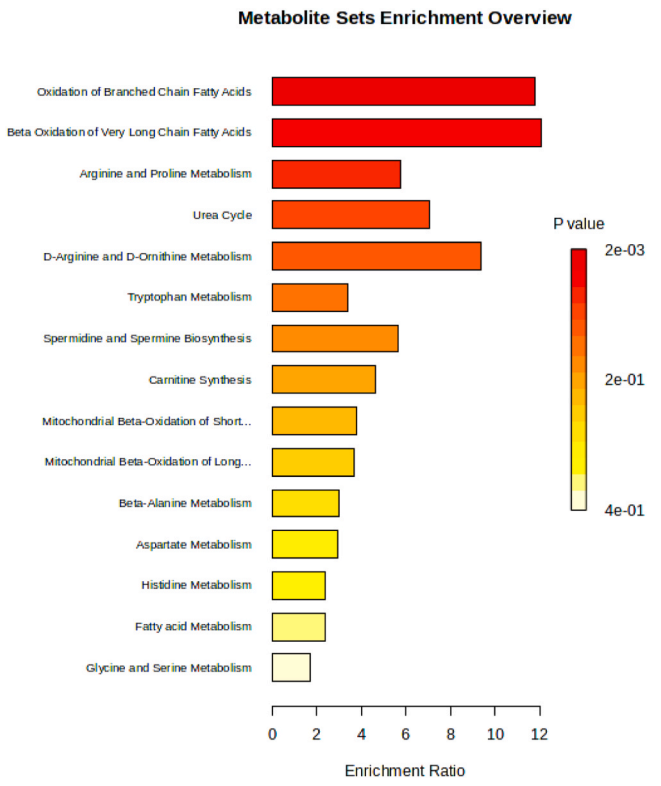

Fig. 5. Pathway enrichment analysis of tissue samples comparing ABT EcN vs ABT PBS.

Arginine and Proline Metabolism, D-Arginine and D-Ornithine Metabolism, Tryptophan Metabolism, Betaine Metabolism, Oxidation of Branched Chain Fatty Acids, and the Urea Cycle. Additional pathways uniquely affected in this comparison include Alanine Metabolism, Glutathione Metabolism, Ammonia Recycling, Porphyrin Metabolism, Glutamate Metabolism, Carnitine Synthesis, Bile Acid Biosynthesis, and Purine Metabolism, highlighting microbial modulation of a broader metabolic network in the absence of antibiotic-induced microbiome depletion.

Enrichment analysis of tumor tissue samples from mice treated with intranasal EcN compared to PBS shows significant metabolic alterations primarily in Oxidation of Branched Chain Fatty Acids, Urea Cycle, Beta Oxidation of Very Long Chain Fatty Acids, and Arginine and Proline Metabolism. Tryptophan Metabolism and Beta-Alanine Metabolism also show significance (raw p-value < 0.05) specifically in this non-antibiotic group, suggesting localized microbial effects on amino acid and lipid metabolism within tumor tissues.

This figure depicts metabolic pathway changes in homogenate samples from antibiotic-treated mice following EcN administration. Pathways significantly enriched (raw p-value < 0.05) include those also seen in the non-antibiotic group—Spermidine and Spermine Biosynthesis, Methionine Metabolism, Glycine and Serine Metabolism, Arginine and Proline Metabolism, D-Arginine and D-Ornithine Metabolism, Tryptophan Metabolism, Betaine Metabolism, Oxidation of Branched Chain Fatty Acids, and Urea Cycle—suggesting a core microbiota-independent response. Uniquely enriched pathways in the antibiotic group include Thyroid Hormone Synthesis, Catecholamine Biosynthesis, Tyrosine Metabolism, Valine, Leucine and Isoleucine Degradation, Phenylalanine and Tyrosine Metabolism, and Propanoate Metabolism, indicating antibiotic pre-treatment may unmask distinct host-microbial metabolic interactions.

In tumor tissue from antibiotic-treated mice, EcN administration led to significant enrichment in Oxidation of Branched Chain Fatty Acids, Urea Cycle, Beta Oxidation of Very Long Chain Fatty Acids, and Arginine and Proline Metabolism—mirroring the non-antibiotic tissue profile. However, pathways such as Tryptophan Metabolism and Beta-Alanine Metabolism, which were significant without antibiotics, do not reach significance here. These findings suggest that while certain EcN-induced metabolic shifts persist regardless of microbiota status, others may depend on the presence of a complex endogenous microbiome.

To narrow down the effects of the EcN treatment (with and without added antibiotics), Volcano plots were calculated. When only adding EcN to the cells – when compared to PBS as control – Carnosine, Kyneurine and the ratios of Putrescine divided by Ornithine and Kyneurine divided by Tryptophan are downregulated by fold changes (EcN vs PBS direction, Fig. 6 and Supp.Table 6).

When comparing the differences in metabolite concetrations of tumor cell homogenates or the tissue samples themselves, which have been respectively treated with a combination of antibiotic and EcN or a combination of PBS and an antibiotic, the following changes can be observed for tissue and homogenate samples respectively:

4. Discussion

Despite the advancements made in the diagnosis and treatment of advanced cancers, the overall outcomes for patient treatment have not significantly improved in recent years. Consequently, it is essential to develop new therapies that may also function synergistically alongside conventional treatments.

Escherichia coli Nissle 1917 (EcN) has emerged as a promising platform for bacterium-mediated cancer therapy, functioning as a "living drug" capable of modulating tumor metabolism and immune responses. Its favorable safety profile, tumor selectivity, and amenability to genetic engineering confer substantial translational potential. In preclinical syngeneic and xenograft models, including 4T1 breast, MC38 colon, and LLC lung tumors, engineered EcN strains have reduced tumor burden by 30–80 %, primarily through arginine pathway modulation, with high tumor colonization rates (>90 %) and persistence for up to two weeks. EcN's Generally Recognized as Safe (GRAS) status, lack of virulence factors, and tolerability following intravenous or intranasal administration further support its clinical viability. Advances in synthetic biology, including CRISPR-based manipulation of arginine metabolism, enhance its therapeutic precision and manufacturability. Moreover, ASS1-deficient tumors—comprising approximately 30–50 % of solid cancers—represent a biomarker-defined subgroup potentially responsive to EcN-based interventions, which can be monitored through imaging and metabolomic profiling. By enabling localized and sustained arginine modulation, EcN may complement systemic depletion therapies such as ADI-PEG20 and pegylated arginase, overcoming their limitations of short half-life and immune resistance. Collectively, these attributes position EcN as a next-generation metabolic biotherapeutic with strong translational promise, now progressing toward phase I clinical evaluation [26–28].

In the previous studies, it was reported that EcN exerts its antitumor effects through a multifaceted reprogramming of arginine metabolism within the tumor microenvironment (TME), enabled by its facultative anaerobic nature and preferential colonization of hypoxic tumor regions. This selective tumor tropism, established in multiple preclinical models, reflects EcN's capacity to adapt metabolically to nutrient-deprived and acidic tumor milieus enriched in lactate and ammonia, facilitating sustained intratumoral persistence without significant off-target colonization. In addition, EcN acts as a dynamic metabolic modulator rather than a passive colonizer. In its depletion mode, EcN consumes arginine and related metabolites through arginase-like activity and substrate competition, perturbing the urea cycle and polyamine synthesis—key anabolic pathways supporting tumor proliferation. These shifts are reflected in elevated ADMA/arginine and putrescine/ornithine ratios, consistent with a state of metabolic stress and disrupted protein synthesis in ASS1-deficient tumors. In contrast, engineered EcN strains can redirect nitrogen flux toward arginine biosynthesis, recycling

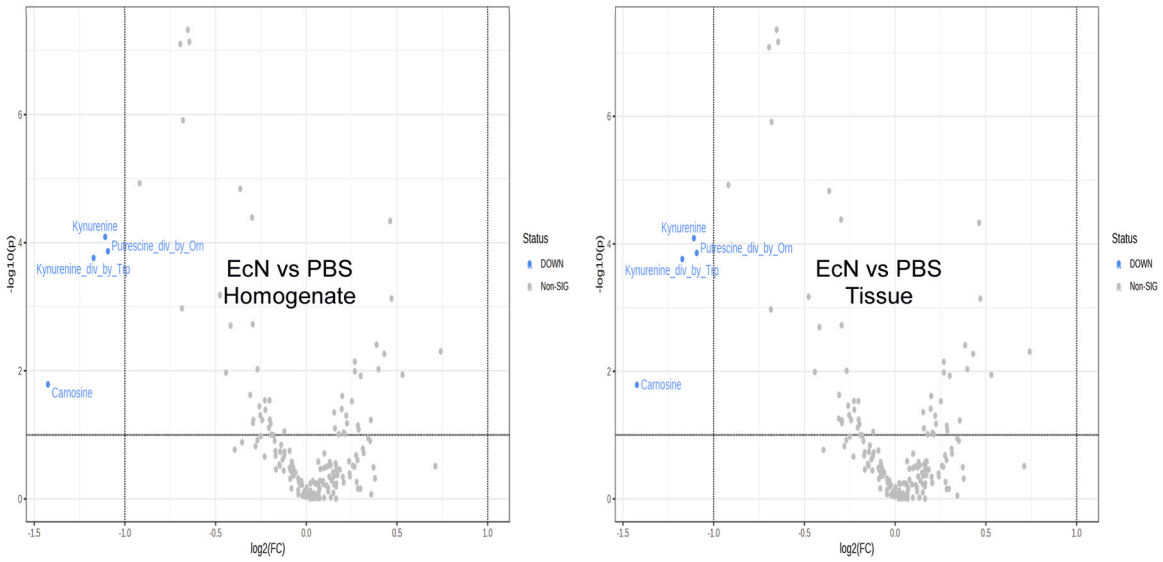

Fig. 6. Volcano plot of EcN vs PBS treatment of cancer cells with apparent status of "down" for Carnosine, Kyneurine and the ratios of Putrescine divided by Ornithine and Kyneurine divided by Tryptophan.

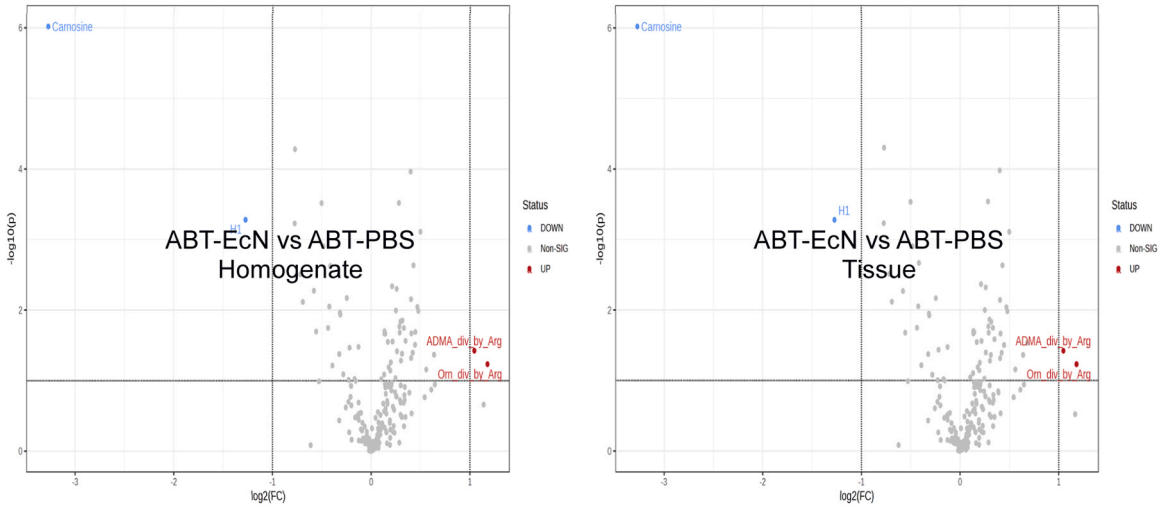

Fig. 7. Volcano plot of a combination of antibiotic and EcN vs a combination of antibiotic and PBS treatment of cancer cells with apparent status of "down" for Carnosine and sugars (H1) and "up" for ratios of ADMA divided by Arginine and Ornithine divided by Arginine.

tumor-derived ammonia via urea cycle enzymes to locally restore arginine levels. This metabolic repletion enhances T-cell receptor signaling through CD3ζ phosphorylation and attenuates the suppressive activity of myeloid-derived suppressor cells, effectively coupling metabolic remodeling with immune activation. Beyond arginine metabolism, EcN also influences interconnected pathways such as arginine–proline cycling and tryptophan catabolism, resulting in reduced kynurenine accumulation and a dampened inflammatory phenotype. Together, these findings position EcN as a mechanistically versatile "metabolic switch" within the TME—capable of either depriving tumors of essential metabolites or restoring them to promote antitumor immunity—underscoring its translational potential as a precision-engineered microbial therapeutic [16,25,28]

In this study, antibiotic-induced microbiome depletion and intranasal EcN administration were employed as complementary preclinical models to probe the host–microbe–tumor axis. While these approaches are not mechanistically connected, their side-by-side application enables differentiation between metabolic effects arising from endogenous microbial communities and those driven by an exogenously introduced probiotic strain. Microbiome depletion establishes a host baseline largely independent of commensal influence, whereas EcN treatment introduces a defined bacterial stimulus capable of modulating tumor metabolism through systemic or immune-mediated pathways. This comparative framework, although exploratory, provides valuable insight into how microbial perturbations—either through loss of the native gut flora or targeted bacterial exposure—can reshape tumor metabolic networks and potentially inform bacterium-mediated cancer therapies.

In our experimental design, the intranasal route was selected for E. coli Nissle (EcN) administration to optimize systemic delivery and reduce potential confounding factors associated with oral dosing. Intranasal application enables EcN to access the respiratory tract and potentially enter systemic circulation more rapidly than oral administration, facilitating direct interaction with the host immune system and tumor microenvironment while bypassing extensive gut colonization and immune filtering. This approach was particularly important for distinguishing the systemic metabolic effects of EcN from those arising due to gut microbiota modulation. By minimizing gastrointestinal

involvement, we ensured that observed metabolic changes could be attributed primarily to EcN's systemic influence rather than secondary effects of intestinal colonization or microbiome reshaping. Additionally, intranasal delivery provides controlled and reproducible bacterial exposure, avoiding degradation by gastric acid or digestive enzymes that can occur during oral delivery. Thus, the intranasal route served as a proof-of-concept for a non-oral, microbiome-based therapeutic approach, allowing us to assess EcN's capacity to modulate tumor metabolism in a preclinical translational context [28,36]

Arginine depletion is a well-supported potential therapeutic strategy for cancer, grounded in the metabolomic vulnerabilities of many tumors and their established ties to core cancer biology principles such as metabolic reprogramming, auxotrophy, and immune modulation. I analysed 10 studies (including preclinical models, phase I-III trials, and systematic reviews) across cancers like melanoma, hepatocellular carcinoma (HCC), prostate, mesothelioma, and others, highlighting how arginine depletion exploits these links.

Arginine depletion represents a promising therapeutic avenue in oncology, leveraging fundamental metabolic vulnerabilities rooted in cancer biology. Many tumors display arginine auxotrophy due to the silencing or reduced expression of argininosuccinate synthetase 1 (ASS1), a key enzyme in the urea cycle required for de novo arginine synthesis. This deficiency renders tumor cells dependent on extracellular arginine, and its depletion disrupts essential biosynthetic and signaling pathways—including protein synthesis, nitric oxide, and polyamine metabolism—integral to tumor proliferation, metabolic reprogramming, and mTOR activation. Epigenetic suppression of ASS1, observed in a high proportion of melanomas, mesotheliomas, and hepatocellular carcinomas, further amplifies this vulnerability. Evidence from preclinical models and clinical trials (phases I–III) supports that arginine deprivation not only induces tumor cell apoptosis, autophagy, and senescence but also reshapes the tumor microenvironment by inhibiting angiogenesis and enhancing immune responsiveness, such as increasing T-cell infiltration and reducing myeloid-derived suppressor cells. Moreover, ASS1 expression has emerged as a reliable biomarker for treatment response, with low ASS1 levels correlating with objective response rates of 25–47 % in early-phase studies. Collectively, these findings underscore the translational potential of arginine depletion as a metabolically targeted, biomarker-driven strategy that aligns with contemporary principles of precision oncology [37–41]

In this metabolomics study we compared metabolite profiles in cancer tissues of 4T1 syngeneic tumor bearing mice after temporal antibiotic-induced depletion of the gut microbiome and/ or intranasal Escherichia coli Nissle 1917 (EcN) treatments. In general, the role of gut bacteria in modulating the anticancer response is a controversial topic [30]. However, it is known that several different gut bacteria positively influence tumor treatment, but no studies have identified the corresponding mechanism until now. Interestingly, after depletion of the gut microbiome by antibiotics, both antitumoral and protumoral activity have been described [32–35,42,43].

Our results demonstrated wide variation in metabolomics and pathways in tumors of four different treated groups (ABT EcN, EcN, ABT PBS, PBS). Both tissue or homogenate samples (with or without antibiotics) enrichment analyzes have shown that the EcN groups (ABT EcN, EcN) have the most changed metabolites and pathways compared to PBS control groups (ABT PBS, PBS). In addition, the homogenate samples show also a rather similar pattern, however there are some more differences between the pathway analyses of the antibiotic and non-antibiotic groups. The Spermidine and Spermine Biosynthesis, Methionine Metabolism, Glycine and Serine Metabolism, Arginine and Proline Metabolism, D-Arginine and D-Ornithine Metabolism, Tryptophan Metabolism, Betaine Metabolism, Oxidation of Branched Chain Fatty Acids and Urea Cycle are similarly found to be significantly affected in both groups by their raw p-value. However Alanine Metabolism, Glutathione Metabolism, Ammonia Recycling, Porphyrin Metabolism, Glutamate Metabolism, Carnitine Synthesis, Bile Acid Biosynthesis and Purine Metabolism are only found to be below 0.05 in the raw p-value in the homogenate samples without antibiotic, whereas Thyroid hormone synthesis, Catecholamine Biosynthesis, Tyrosine Metabolism, Valine, Leucine and Isoleucine Degradation, Phenylalanine and Tyrosine Metabolism and Propanoate Metabolism are exclusively below 0.05 (raw p-value) for the homogenate samples with antibiotics.

For pairings of ABT EcN vs ABT PBS and EcN vs PBS, we found statistically significant metabolite changes in the Oxidation of Branched Chain Fatty Acids, Urea Cycle, Beta Oxidation of Very Long Chain Fatty Acids, Arginine and Proline Metabolism in the tissue tumor samples (Table1). The Tryptophan Metabolism and the Beta-Alanine Metabolism show a raw p-value of < 0.05 in the tissue samples without antibiotics only.

previous studies investigated the potential effects of branched-chain fatty acids (BCFAs) and their oxidation on cancer. A 2018 study from [44] found that the BCFA isovaleryl-CoA promotes the growth of breast cancer cells by activating a signalling pathway involved in cell proliferation and survival, whereas a comparative study from 2004 has shown that some BCFAs have the exact opposite mode of action: they are cytotoxic to breast cancer cells [45]

Arginine is an amino acid that plays a crucial role in cellular metabolism and growth. Deprivation of arginine has been investigated as a potential therapeutic strategy for cancer treatment [46,47].

One early example of an argininase deprivation therapy is pegylated arginine deiminasepegylated recombinant human arginase 1 (Peg-rhArg1), which is a modified enzyme that degrades arginine and was evaluated in clinical trials for the treatment of hepatocellular carcinoma [46].

5. Conclusion

Overall, arginine deprivation is an active area of research in the field of cancer therapy. If Arginine depletion in cancer cells can be induced by a combination of EcN mixed with an antibiotic, it could indeed be a promising new avenue as a potential therapeutic strategy for the future.

Ethical Approval and Consent to participate

Animal experiments were carried out in accordance with the protocol approved by the Government of Upper Franconia, Germany, according to the guidelines for the welfare and use of animals in cancer research (application No.: RUF-55.2.2.–2532–2–849).

Consent for publication

Hereby, the authors provide consent for the publication of the manuscript detailed above, including any accompanying images or data contained within the manuscript

Funding

Not applicable

CRediT authorship contribution statement

Cornelia Prehn: Writing – review & editing, Investigation. **Ivaylo Gentschev:** Writing – original draft, Methodology, Investigation, Conceptualization. **Michael Witting:** Writing – review & editing, Conceptualization. **Stefanie Hauck:** Writing – original draft, Conceptualization. **Mingyu Ye:** Methodology. **Ivan Petrov:** Methodology, Investigation. **Aladar A. Szalay:** Writing – review & editing, Supervision, Resources, Funding acquisition, Conceptualization. **Eman M. Othman:** Writing – review & editing, Validation. **Alexander Cecil:** Writing – original draft, Validation, Methodology, Investigation, Conceptualization.

Declaration of Competing Interest

The authors declare that they have no known competing financial interests or personal relationships that could have appeared to influence the work reported in this paper.

Appendix A. Supporting information

Supplementary data associated with this article can be found in the online version at doi:10.1016/j.biopha.2025.118750.

Data availability

No data was used for the research described in the article.

References

[1] K.D. Miller, et al., Cancer treatment and survivorship statistics, 2022. CA Cancer J. Clin. 72 (5) (2022) 409–436.
[2] M. Luo, et al., Bacteria-mediated cancer therapy: a versatile bio-sapper with translational potential, Front Oncol. 12 (2022) 980111.
[3] J.Y. Fan, et al., Bacteria in cancer therapy: A new generation of weapons, Cancer Med 11 (23) (2022) 4457–4468.
[4] Y.F. Mustafa, When the gut Speaks: The hidden toll of irritable bowel syndrome on body and mind, Gastroenterol. Endosc. 3 (3) (2025) 135–151.
[5] J. Tjuvajev, et al., Salmonella-based tumor-targeted cancer therapy: tumor amplified protein expression therapy (TAPET) for diagnostic imaging, J. Control Release 74 (1-3) (2001) 313–315.
[6] T. Sasaki, et al., Genetically engineered Bifidobacterium longum for tumor-targeting enzyme-prodrug therapy of autochthonous mammary tumors in rats, Cancer Sci. 97 (7) (2006) 649–657.
[7] Y.A. Yu, et al., Visualization of tumors and metastases in live animals with bacteria and vaccinia virus encoding light-emitting proteins, Nat. Biotechnol. 22 (3) (2004) 313–320.
[8] L.M. Wood, et al., Cancer immunotherapy using Listeria monocytogenes and listerial virulence factors, Immunol. Res 42 (1-3) (2008) 233–245.
[9] N. Agrawal, et al., Bacteriolytic therapy can generate a potent immune response against experimental tumors, Proc. Natl. Acad. Sci. USA 101 (42) (2004) 15172–15177.
[10] J. Theys, et al., Repeated cycles of Clostridium-directed enzyme prodrug therapy result in sustained antitumour effects in vivo, Br. J. Cancer 95 (9) (2006) 1212–1219.
[11] M.T. Duong, et al., Bacteria-cancer interactions: bacteria-based cancer therapy, Exp. Mol. Med 51 (12) (2019) 1–15.
[12] J.M. Pawelek, K.B. Low, D. Bermudes, Bacteria as tumour-targeting vectors, Lancet Oncol. 4 (9) (2003) 548–556.
[13] S. Zhou, et al., Tumour-targeting bacteria engineered to fight cancer, Nat. Rev. Cancer 18 (12) (2018) 727–743.
[14] Q. Liu, et al., Escherichiacoli Nissle 1917 as a Novel Microrobot for Tumor-Targeted Imaging and Therapy, Pharmaceutics 13 (8) (2021).
[15] B.J. Rembacken, et al., Non-pathogenic Escherichia coli versus mesalazine for the treatment of ulcerative colitis: a randomised trial, Lancet 354 (9179) (1999) 635–639.
[16] A. Chmielewska, H. Szajewska, Systematic review of randomised controlled trials: probiotics for functional constipation, World J. Gastroenterol. 16 (1) (2010) 69–75.
[17] H.A. Malchow, Crohn's disease and Escherichia coli. A new approach in therapy to maintain remission of colonic Crohn's disease? J. Clin. Gastroenterol. 25 (4) (1997) 653–658.
[18] M.R. Barbaro, et al., Escherichia coli Nissle 1917 restores epithelial permeability alterations induced by irritable bowel syndrome mediators, Neurogastroenterol. Motil. (2018) e13388.
[19] V.M. Isabella, et al., Development of a synthetic live bacterial therapeutic for the human metabolic disease phenylketonuria, Nat. Biotechnol. 36 (9) (2018) 857–864.
[20] B. Ou, et al., Genetic engineering of probiotic Escherichia coli Nissle 1917 for clinical application, Appl. Microbiol Biotechnol. 100 (20) (2016) 8693–8699.
[21] K. Gronbach, et al., Safety of probiotic Escherichia coli strain Nissle 1917 depends on intestinal microbiota and adaptive immunity of the host, Infect. Immun. 78 (7) (2010) 3036–3046.
[22] J. Stritzker, et al., Tumor-specific colonization, tissue distribution, and gene induction by probiotic Escherichia coli Nissle 1917 in live mice, Int J. Med Microbiol 297 (3) (2007) 151–162.
[23] J. Stritzker, et al., Enterobacterial tumor colonization in mice depends on bacterial metabolism and macrophages but is independent of chemotaxis and motility, Int J. Med Microbiol 300 (7) (2010) 449–456.
[24] K. Westphal, et al., Containment of tumor-colonizing bacteria by host neutrophils, Cancer Res 68 (8) (2008) 2952–2960.
[25] Y. Zhang, et al., Escherichia coli Nissle 1917 targets and restrains mouse B16 melanoma and 4T1 breast tumors through expression of azurin protein, Appl. Environ. Microbiol 78 (21) (2012) 7603–7610.
[26] D.S. Leventhal, et al., Immunotherapy with engineered bacteria by targeting the STING pathway for anti-tumor immunity, Nat. Commun. 11 (1) (2020) 2739.
[27] A. Altenhoefer, et al., The probiotic Escherichia coli strain Nissle 1917 interferes with invasion of human intestinal epithelial cells by different enteroinvasive bacterial pathogens, FEMS Immunol. Med Microbiol 40 (3) (2004) 223–229.
[28] I. Gentschev, et al., Tumor Colonization and Therapy by Escherichia coli Nissle 1917 Strain in Syngeneic Tumor-Bearing Mice Is Strongly Affected by the Gut Microbiome, Cancers (Basel) 14 (24) (2022).
[29] R. Sender, S. Fuchs, R. Milo, Revised Estimates for the Number of Human and Bacteria Cells in the Body, PLoS Biol. 14 (8) (2016) e1002533.
[30] W.Y. Cheng, C.Y. Wu, J. Yu, The role of gut microbiota in cancer treatment: friend or foe? Gut 69 (10) (2020) 1867–1876.
[31] E.K. Costello, et al., The application of ecological theory toward an understanding of the human microbiome, Science 336 (6086) (2012) 1255–1262.
[32] A. Aghamajidi, S. Maleki Vareki, The Effect of the Gut Microbiota on Systemic and Anti-Tumor Immunity and Response to Systemic Therapy against Cancer, Cancers (Basel) 14 (15) (2022).
[33] D.H. Reikvam, et al., Depletion of murine intestinal microbiota: effects on gut mucosa and epithelial gene expression, PLoS One 6 (3) (2011) e17996.
[34] A. Zarrinpar, et al., Antibiotic-induced microbiome depletion alters metabolic homeostasis by affecting gut signaling and colonic metabolism, Nat. Commun. 9 (1) (2018) 2872.
[35] S. Zukunft, et al., High-throughput extraction and quantification method for targeted metabolomics in murine tissues, Metabolomics 14 (1) (2018) 18.
[36] P.J. Sarate, et al., Correction: E. coli Nissle 1917 is a safe mucosal delivery vector for a birch-grass pollen chimera to prevent allergic poly-sensitization, Mucosal Immunol. 12 (1) (2019) 291.
[37] B. Delage, et al., Arginine deprivation and argininosuccinate synthetase expression in the treatment of cancer, Int J. Cancer 126 (12) (2010) 2762–2772.
[38] C. Riess, et al., Arginine-Depleting Enzymes - An Increasingly Recognized Treatment Strategy for Therapy-Refractory Malignancies, Cell Physiol. Biochem 51 (2) (2018) 854–870.
[39] C.L. Chen, et al., Arginine Signaling and Cancer Metabolism, Cancers (Basel) 13 (14) (2021).
[40] M.M. Phillips, M.T. Sheaff, P.W. Szlosarek, Targeting arginine-dependent cancers with arginine-degrading enzymes: opportunities and challenges, Cancer Res Treat. 45 (4) (2013) 251–262.
[41] S. Zou, et al., Arginine metabolism and deprivation in cancer therapy, Biomed. Pharm. 118 (2019) 109210.
[42] Z. Pang, et al., Using MetaboAnalyst 5.0 for LC-HRMS spectra processing, multi-omics integration and covariate adjustment of global metabolomics data, Nat. Protoc. 17 (8) (2022) 1735–1761.
[43] J. Kim, H.K. Lee, The Role of Gut Microbiota in Modulating Tumor Growth and Anticancer Agent Efficacy, Mol. Cells 44 (5) (2021) 356–362.
[44] J.V. Lee, et al., Acetyl-CoA promotes glioblastoma cell adhesion and migration through Ca(2+)-NFAT signaling, Genes Dev. 32 (7-8) (2018) 497–511.
[45] S. Wongtangtintharn, et al., Effect of branched-chain fatty acids on fatty acid biosynthesis of human breast cancer cells, J. Nutr. Sci. Vitam. (Tokyo) 50 (2) (2004) 137–143.
[46] L. Feun, et al., Arginine deprivation as a targeted therapy for cancer, Curr. Pharm. Des. 14 (11) (2008) 1049–1057.
[47] L.G. Feun, M.T. Kuo, N. Savaraj, Arginine deprivation in cancer therapy, Curr. Opin. Clin. Nutr. Metab. Care 18 (1) (2015) 78–82.